

# Voice-Face Homogeneity Tells Deepfake

Harry Cheng<sup>1</sup>, Yangyang Guo<sup>2\*</sup>, Tianyi Wang<sup>3</sup>, Qi Li<sup>1</sup>, Tao Ye<sup>1</sup>, Liqiang Nie<sup>1\*</sup>

<sup>1</sup>Shandong University <sup>2</sup>National University of Singapore <sup>3</sup>The University of Hong Kong

## Abstract

Detecting forgery videos is highly desired due to the abuse of deepfake. Existing detection approaches contribute to exploring the specific artifacts in deepfake videos and fit well on certain data. However, the growing technique on these artifacts keeps challenging the robustness of traditional deepfake detectors. As a result, the development of generalizability of these approaches has reached a blockage. To address this issue, given the empirical results that the identities behind voices and faces are often mismatched in deepfake videos, and the voices and faces have homogeneity to some extent, in this paper, we propose to perform the deepfake detection from an unexplored voice-face matching view. To this end, a voice-face matching detection model is devised to measure the matching degree of these two on a generic audio-visual dataset. Thereafter, this model can be smoothly transferred to deepfake datasets without any fine-tuning, and the generalization across datasets is accordingly enhanced. We conduct extensive experiments over two widely exploited datasets - DFDC and FakeAVCeleb. Our model obtains significantly improved performance as compared to other state-of-the-art competitors and maintains favorable generalizability. The code has been released at <https://github.com/xaCheng1996/VFD>.

## 1. Introduction

Deepfake [18, 23, 34] is to synthesize the media in which a person is replaced with someone else's likeness. Given its successful application in animation [39] and online education [38], deepfake has attracted increasing interest from academic and industrial practitioners. However, the abuse of such techniques, such as maliciously editing porn and violent videos<sup>1</sup>, seriously challenges social functioning and ethics, garnering widespread concerns. It is hence imperative to detect deepfake abuse with effective measures.

Considerable research efforts have been dedicated to detecting deepfakes thus far [28, 40, 41, 49]. Most of them

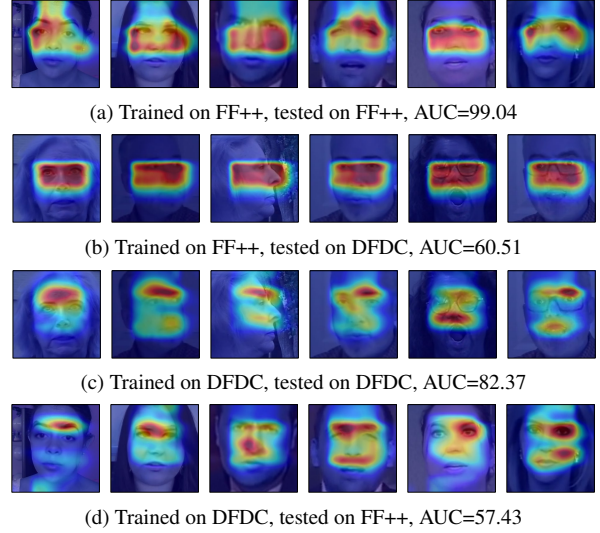


Figure 1. Heat maps and AUC scores (%) from Xception [41] under different settings. When trained on the FF++, the attention is mostly placed on the eyes regions, and is shifted to the forehead and nose for DFDC. Since the editing algorithm focuses on different regions with respect to distinctive data, a well-trained model thus cannot adapt smoothly across datasets.

explore the face manipulation artifacts of fake videos, including the visual artifacts from face attentive regions [51], apparent changes in the frequency domain resulting from up-sampling [27], or emotional biases caused by the forgery face [30]. Nevertheless, these methods are all limited by one critical downside, namely, *inferior generalization across datasets*. For instance, a model trained on the DFDC dataset [8] suffers significant performance degradation when migrated to other deepfake datasets (e.g., FF++ [41] or Celeb-DF [26]). The key reason is that different datasets are built with distinctive algorithms. As a result, previous detection approaches tend to fit well on the specific training data, and the generalization is thereby hampered. For instance, Figure 1 illustrates that the models trained on FF++ pay more attention to the eyes yet fail on DFDC since the salient regions are instead the forehead and nose.

One most practical manner of dealing with this setting, namely cross-dataset detection, is extending current datasets with specialized auxiliary data, e.g., blending re-

\*Corresponding author: Yangyang Guo and Liqiang Nie.

<sup>1</sup><https://www.bbc.com/news/technology-42912529>.

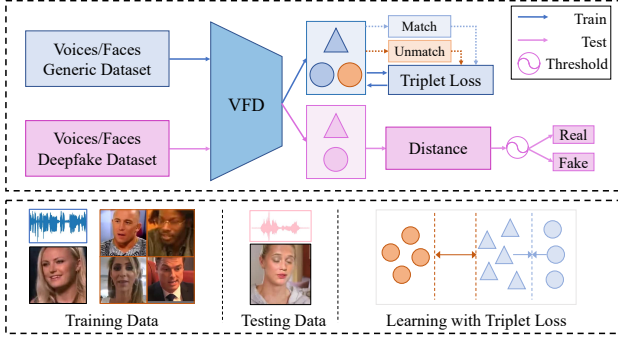


Figure 2. Schematic illustration of our proposed VFD model. We adopt the triplet loss to pull matched voices (blue triangles) and faces (blue circles) closer while pushing unmatched faces (orange circles) faraway. The model is trained on generic audio-visual data without any manipulation from deepfake, and evaluated on various deepfake datasets.

gion [25], or lip movement [14]. Nevertheless, constructing such datasets is time-consuming, and the models often require computationally intensive pre-training and fine-tuning to characterize complementary features of these data. In addition, the performance of these approaches remains sub-optimal, as observed in our experiments. We hence consider to address this task from an unexplored angle.

Our solution is inspired by the recent progress from cross-modal biometric matching [31, 35], which certifies the fact that a single person’s voices and faces are strongly correlated. Based upon this finding, we perform an in-depth analysis of the existing deepfake algorithms and recognize a serious voice-face mismatching problem. For example, an edited face of President Obama can be matched with the voice of President Reagan. This motivates us to speculate - Can we perform deepfake detection from a discrimination view of voices and faces?

To answer this question, we tentatively propose a simple method called Voice-Face matching Detection, VFD for short. In particular, we perform matching between voices and faces rather than directly attacking the artifacts from deepfake. An overview of VFD is shown in Figure 2. We first train VFD on a generic audio-visual dataset (such as Voxceleb2 [7]) without being manipulated by deepfake algorithms. Specifically, given an anchor voice clip, the triplet loss [15] is employed to pull matched voice clip and face instances closer while pushing unmatched ones further. Thereafter, we directly transfer this model to detect forgery videos without any fine-tuning. Notably, the deepfake data are agnostic to the training of VFD, thus avoiding any over-fitting on deepfake features, and the model’s generalizability over various deepfake datasets is thereby guaranteed. Besides, the VFD alleviates the limitation of auxiliary data or fine-grained deepfake artifacts, which serves as another merit.

We conduct extensive experiments over two widely ex-

ploited deepfake datasets - DFDC and FakeAVCeleb [19]. The results demonstrate that our VFD model yields superior performance compared to baselines, with AUCs of 98.45% and 96.72% upon DFDC and FakeAVCeleb, respectively. As a side product, our VFD achieves a new state-of-the-art on these two benchmarks.

The main contributions of this work are three-fold:

- We address the deepfake detection from a voice-face matching view. To the best of our knowledge, we are the first to perform cross-dataset deepfake detection excluding any additional auxiliary data.
- We devise a simple yet effective multi-modal fusion matching framework to justify real and fake videos. Our model requires only human-speaking data and eases the suffering of fine-tuning on various deepfake datasets. In this way, the effectiveness is ensured without the detriment of any updates from deepfake algorithms.
- The experimental results show that our model outperforms a variety of SOTA competitors with a large margin.

## 2. Related Work

### 2.1. Deepfake

Benefiting from the continuous development of portrait synthesis, deepfake has recently emerged as a prevailing research problem. Existing algorithms either leverage the image only or the 3D information to edit videos. The image only methods synthesize fake faces for the target identities, which are then blended into the given video [2]. For example, Li *et al.* [24] utilized cascaded AAD blocks to integrate identities and face attributes within multiple feature levels, and realistic human faces can then be generated. Wav2Lip [38] synthesizes accurate speaking videos driven by speeches and the upper face. Different from these methods, Kim *et al.* [20] applied 3DMM [3] to produce the portraits with controllable poses. HifiFace [45] generates photo-realistic videos via the 3D shape-aware identity extractor. However, the existing deepfake approaches pay much attention to the face regions while the voice-face consistency is hard to be maintained.

### 2.2. Deepfake Detection

Deepfake detection is often cast as a binary (real or fake) classification task. Preliminary efforts often endeavor to detect the specific traces of manipulation [40, 41]. Masi *et al.* [28] proposed a two-branch network to separately extract artifacts of color and frequency domains [27]. SSTNet [49] detects edited faces through spatial, steganalysis, and temporal features. In contrary to these approaches utilizing the vision modality only, studies nowadays exploit

the multi-modal information [11, 46] for deepfake detection [36, 50, 51]. For instance, lip-syncing and dubbing models [22] are employed to identify the audio-visual inconsistency from a speaker. Hou *et al.* [52] predicted the probability of voices and faces being edited to judge the video credibility. Mittal *et al.* [30] extracted the emotional biases that video and audio jointly mention, based on which the detection objective can be achieved. Previous approaches have gained certain improvements on some datasets. Nonetheless, when transferring to unknown data, inferior performance is often confronted.

To address this lack of generalization issue, several cross-dataset detection approaches are proposed. Li *et al.* [25] constructed auxiliary data from extracted blending regions in large-scale videos to enhance the robustness. Haliassos *et al.* [14] utilized a pre-trained lip-reading model to explore the irregularities in mouth movements, followed by delicate fine-tuning on the forgery data. Nonetheless, these methods always require auxiliary data and yield increased training overload. In this work, we propose to tackle deepfake detection from a novel matching view. Specifically, the matching between voices and faces is taken as the proxy for discriminating real and fake videos, since the voices and faces show a severe mismatch from deepfake algorithms. Our method exhibits promising generalization over various deepfake datasets, which requires only paired voices and faces for training.

### 2.3. Cross-modal Biometric Matching

Cross-modal biometric matching aims to retrieve the corresponding video for a given audio from multiple candidates, or vice versa [31]. Among the initial efforts, researchers extracted video and audio features via pre-trained models and then employed cross entropy [31] or cosine loss [12, 16] to measure the matching degree. Later studies take into consideration the interactions among different modalities. For instance, Wen *et al.* [47] devised a two-level loss, which leverages both local and global features on modality alignment. ADSM [6] adopts an adversarial matching network to extract the high-level semantical features. A specially designed discriminator is then employed to bridge the voice and face gap while maintaining semantic consistency. Moreover, Speech2Face [35] applies a pre-trained face decoder network to reconstruct the face from speech clips. The methods in this category, indeed provide certain support that the voices and faces from the same person are strongly correlated [5].

## 3. Methodology

In this section, we first present the evidence from two aspects for the intuition of our method, followed by the detailed introduction of our multi-modal matching model

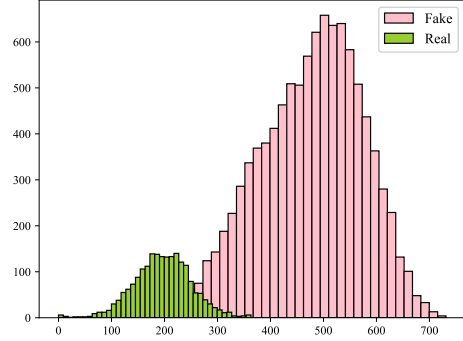


Figure 3. The distances between voices and faces in real (green) and fake (pink) videos. The x-axis represents the distance values, and the y-axis is the number of videos.

trained on generic audio-visual data. We end this section with the application on downstream deepfake datasets.

### 3.1. Method Intuition

Research on human perception and neurology have shown that humans can outline pictures of a person’s appearance based on the voices, or vice versa [17]. That is, voices and faces exhibit a high degree of homogeneity in the human brain and are associated closely with identities. In light of this, we contribute to exploring whether the matching between these two can serve as a proxy in detecting deepfake. To this end, we perform some probing tests, which mainly answer the following two questions:

- **Q1:** Are the voices and faces matched in deepfake videos?
- **Q2:** Can the voices and faces be leveraged to discriminate different identities?

#### 3.1.1 Voice-Face Mismatching in Deepfake Data (Q1)

We evaluate whether the voices and faces are matched in deepfake videos via measuring the distances between them. In particular, we randomly sample 2,000 real and 10,000 fake videos from DFDC. Two VGG-based [4] models are employed to extract the voice and face features. Thereafter, we calculate the corresponding Euclidean distance between these two sets of features, and display the results in Figure 3.

From this figure, we have the following observations: 1) The voice-face distances in the real videos are much smaller than those in the fake ones (the distance split line is around 270). That is, the voice and face in one real video match better in the feature space, while fake videos demonstrate serious mismatch evidence. And 2) only a small fraction of real videos share similar distances with fake ones, which is due to the presence of the ambient noise during recording.

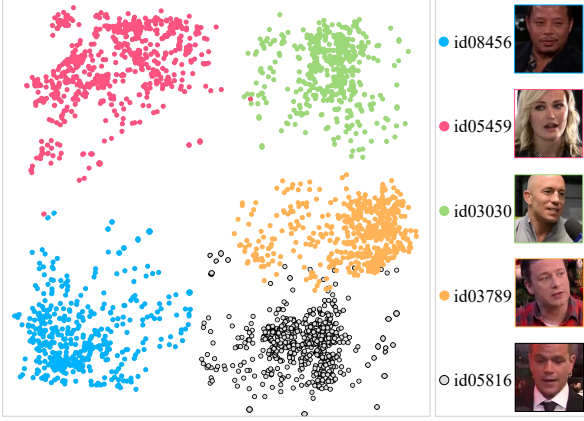


Figure 4. t-SNE [43] visualization of voice features from five identities: *id08456* (blue), *id05459* (pink), *id03030* (green), *id03789* (yellow), and *id05816* (grey).

### 3.1.2 Voice Discrimination over Identities (Q2)

Faces encode essential cues for distinguishing different identities, which have been extensively proven by considerable studies [10, 29, 42]. To testify whether the voices can achieve similar effects, we extract the voice features and cluster them in the following way. We employ the VGG-based model as the backbone and the triplet loss to learn the voice features, where the voice clips from the same identity are deemed as positive and from other identities as negative. In the second step, we randomly sample over 2,000 voice clips from five people in the Voxceleb2 dataset and show the voice feature manifold embedding in Figure 4.

Figure 4 tells that voices from the same identity tend to cluster together with apparent boundaries, demonstrating the discrimination capability of voices. Moreover, the learned features correlate tightly with facial characteristics. For example, *id05459* (pink) is far from the other four identities since she is the only female among the total five persons. Moreover, *id05816* (grey) and *id03789* (yellow) share similar ages (in their 40s), which drives the voice features closer with each other.

## 3.2. Voice-Face Matching Detection Network

Based on the above findings that a single person’s voices and faces have certain homogeneity, in this paper, we propose to detect deepfake videos by judging the matching degree of these two. To achieve this goal, we design a Voice-Face matching Detection network. In particular, our VFD is embodied with a dual-stream network, wherein the voices and faces are separately processed. A matching function is then utilized to determine the matching degree.

As shown in Figure 5a, the proposed VFD follows a Siamese paradigm [13]: the voices and faces are separately consumed to yield identity-sensitive features, and a triplet loss [15] is then employed to achieve the homogeneity be-

tween voices and their matched faces. In what follows, we first present the data preprocessing protocol. After that, we elaborate the overall architecture of our VFD and its corresponding training strategy sequentially.

### 3.2.1 Data Preprocessing

For each input audio  $\mathcal{A}$ , we extract a three-second voice clip with a 16kHz sample rate, which will be represented as a spectrogram  $\mathbf{C} \in \mathcal{R}^{M_c \times H_c \times W_c}$ , where  $M_c$  denotes the channel number,  $H_c$  and  $W_c$  are the height and width of the spectrograms, respectively. On the other hand, for the video input  $\mathcal{V}$ , we randomly leverage one random face frame  $\mathbf{I} \in \mathcal{R}^{M_I \times H_I \times W_I}$  to represent it as each video involves one identity only [7, 8, 19].

The key to perform the triplet loss is to construct efficacious positive and negative samples. In this work, we utilize the voice as the anchor and build <positive, negative> pairs from identity faces<sup>2</sup>. Specifically, for a given voice clip  $\mathbf{C}$ , it is straightforward to sample the faces from the same identity as its positive instances. As to the negative instance sampling, we simply adopt the faces from other identities as the counterpart, while leaving cumbersome hard negative mining as future work. After this, the voice and face features (both positive and negative) are inputted to two independent feature extractors, which is detailed as follows.

### 3.2.2 Voice and Face Feature Extractor

Extracting both voice and face features associated with identity is of vital importance for a multi-modal matching network. To this end, an elaborated multi-modal feature extractor is presented, and the overall architecture is shown in Figure 5b. It is composed of two novel modules, i.e., MMR and IFL, short for multi-modal representation and identity feature learning, respectively. In the following, we take the processing for the face input  $\mathbf{I}$  as an example, and the voice feature extractor is designed in a similar fashion.

**Multi-Modal Representation.** We firstly utilize a deep forward convolutional projection inherits from a well-developed VGG-Face model [37] to extract the initial face features,

$$\mathbf{I}_v(i, j, m) = \sum_{u,v=0}^N \sum_{t=0}^M h(u, v, t) \otimes \mathbf{I}(i-u, j-v, m-t), \quad (1)$$

where  $N$  is the image size (the height and width are identical in face images),  $M$  denotes the output channel number, and  $h(\cdot)$  represents the convolutional kernel. In this manner, we obtain the F-channel feature maps  $\mathbf{I}_v \in \mathcal{R}^{F \times D}$ .

<sup>2</sup>It is also feasible to choose faces as anchors, which will serve as a possible extension of this work.

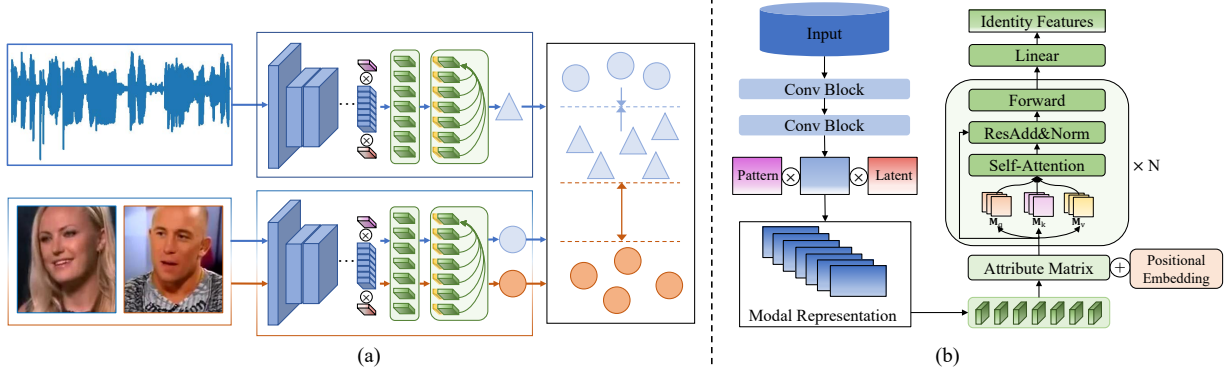


Figure 5. Overall architecture of (a) Siamese voice-face matching network, (b) voice/face feature extractor.

Thereafter, we devise two learnable matrices, namely, the topic pattern matrix  $\mathbf{P} \in \mathcal{R}^{K \times F}$  and the latent representation matrix  $\mathbf{L} \in \mathcal{R}^{D \times S}$ , to filter noise and redundancy of the  $\mathbf{I}_v$ , which has been proven effective in multiple modality information [33]. Each column of the matrix  $\mathbf{P}$  corresponds to one face attribute basis, while that of  $\mathbf{L}$  refers to one aspect of the visual modality in the latent pattern space. These two matrices are then multiplied with  $\mathbf{I}_v$  to obtain the face attribute description matrix  $\mathbf{M}_I \in \mathcal{R}^{K \times S}$ :

$$\mathbf{M}_I = \mathbf{P} \otimes \mathbf{I}_v \otimes \mathbf{L}. \quad (2)$$

Notably, it is non-trivial to learn the overall identity features of voices or faces with the above VGG-based module, as only local information is aggregated by this fashion while ignoring the global context. Therefore, in the next, we develop another novel identity feature learning module to tackle this.

**Identity Feature Learning** is a transformer-like [9, 44] module to learn the identity features based on the initial multi-modal representation from the first module, wherein the unique self-attention mechanism is employed to extract the non-local joint features. To this end, we firstly concatenate a learnable positional encoding  $\mathbf{E}$  to  $\mathbf{M}_I$  for retaining the positional information of the image feature maps:

$$\mathbf{M}_p = \mathbf{M}_I \oplus \mathbf{E}. \quad (3)$$

And then, we map the  $\mathbf{M}_p$  into three attentive matrices:

$$[\mathbf{M}_q, \mathbf{M}_k, \mathbf{M}_v] = [\mathbf{W}_q, \mathbf{W}_k, \mathbf{W}_v] \otimes \mathbf{M}_p, \quad (4)$$

where these three matrices share a similar size of  $\mathcal{R}^{U \times S}$ . We then utilize the self-attention mechanism to perform non-local learning,

$$g(\mathbf{M}_q, \mathbf{M}_k, \mathbf{M}_v) = \text{softmax}\left(\frac{\mathbf{M}_q \mathbf{M}_k^T}{\sqrt{S}}\right) \mathbf{M}_v. \quad (5)$$

We perform this block several times and finally map the outputs of  $g(\cdot, \cdot, \cdot)$  into the  $\mathbf{k}_I \in \mathcal{R}^{Q \times V}$  with a linear transformation. In a similar fashion, the voice branch will transform voice input to  $\mathbf{k}_C$  with the same shape as  $\mathbf{k}_I$ . Note that

due to the modality gap between voices and faces [31], we do not share parameters between these two extractors but instead expect the triplet loss to enhance the homogeneity modeling.

### 3.2.3 Training Protocol

We employ the triplet loss [15] to update the parameters of VFD as follows:

$$L_T = \max\left\{\sum_{i=0}^T (d(\mathbf{k}_C, \mathbf{k}_I^p) - d(\mathbf{k}_C, \mathbf{k}_I^{n_i}) + r), 0\right\}, \quad (6)$$

where  $\mathbf{k}_C$  denotes the learned features of the voice clip  $\mathbf{C}$ ;  $\mathbf{k}_I^p$  corresponds to a positive instance feature extracted from the matched face image  $\mathbf{I}^p$ ;  $\{\mathbf{k}_I^{n_0}, \mathbf{k}_I^{n_1}, \dots, \mathbf{k}_I^{n_T}\}$  are the negative instance features as described in Section 3.2.1;  $r$  represents a margin threshold, and  $d(\cdot, \cdot)$  is defined as:

$$d(\mathbf{x}, \mathbf{y}) = \|\mathbf{x} - \mathbf{y}\|_2, \quad (7)$$

which indicates the distance in the joint space between voices and faces.

By means of calculating the difference between  $d(\mathbf{k}_C, \mathbf{k}_I^p)$  and  $d(\mathbf{k}_C, \mathbf{k}_I^n)$ , VFD pulls the matched voice clip  $\mathbf{k}_C$  and the positive faces  $\mathbf{k}_I^p$  closer while pushing the unmatched negative faces  $\mathbf{k}_I^n$  further. The hyperparameter  $r$  contributes to make the positive and negative instances more separable.

### 3.3. VFD for Deepfake Detection

Based on the aforementioned Siamese architecture, our VFD is trained on a generic audio-visual dataset, such as Voxceleb2 [7]. We then transfer the well-trained VFD model to deepfake videos where voices and faces might be from some mismatched identities. It is worth noting that our method can be directly applied to perform deepfake detection without any fine-tuning, which is distinctive from previous approaches [14] using heavy adaptation tricks. For deepfake data, we adopt a similar strategy as introduced in

Section 3.2.1, i.e., extracting face images  $\mathbf{I}_d$  and voice clips  $\mathbf{C}_d$ , and apply VFD to determine the matchness:

$$\text{Matching} = \begin{cases} \text{True}, & \text{VFD}(\mathbf{C}_d, \mathbf{I}_d) \leq t, \\ \text{False}, & \text{VFD}(\mathbf{C}_d, \mathbf{I}_d) > t, \end{cases} \quad (8)$$

where the  $\text{VFD}(\cdot, \cdot)$  is the distance computed via Equation (7) in the joint latent space; and  $t$  is selected from the validation set. According to Equation (8), the matching result of the  $\mathbf{I}_d$  and  $\mathbf{C}_d$  being *True* denotes a matched voice-face pair, namely, the input video is real. On the contrary, the *False* result corresponds to fake videos edited by deepfake algorithms.

## 4. Experiment

### 4.1. Dataset

We utilized the Voxceleb2 dataset for training our VFD model. Specifically, Voxceleb2 is a generic audio-visual dataset collected from YouTube videos, containing over 1 million utterances of 6,112 celebrities. We randomly sampled 130K videos over all identities due to the computational overhead and split them into training, validation, and testing sets with a ratio of 8:1:1. Thereafter, the two deepfake datasets - DFDC and FakeAVCeleb, are only employed to evaluate the effectiveness of VFD. DFDC contains 23,654 real videos recorded from 960 identities and 104,500 fake videos. Since some videos in this dataset are mixed with the camera holders' voices, we manually filtered 1,700 real videos with corresponding 5,810 fake videos as the testing set. As for FakeAVCeleb, we directly employed the default testing set, composed of 99 real videos and 4,067 fake videos.

### 4.2. Implement Details

We implemented our model with the Pytorch [53]. And the Adam optimizer [21] is adopted with a learning rate of  $2 \times 10^{-4}$  for parameter updating. All model parameters are initialized using a random normal distribution with a mean of 0 and a standard deviation of 0.02. The model is trained up to 10 epochs with a mini-batch size of 1, i.e., it takes as inputs one voice clip at each time. The threshold  $r$  used in Equation (6) is set 50.0, and the  $t$  in Equation (8) is 300.0 as selected in the validation set of Voxceleb2. We used six transformer blocks with 8-head self-attention in each IFL, i.e., the  $N = 6$  in Figure 5b. The input face images are resized to  $224 \times 224$ , while the voice clips are represented as  $512 \times 300$  spectrograms since each second of voice clips are divided into 100 small windows in the sliding window manner.

### 4.3. Compared Baselines and Evaluation Metrics

We compared our model with ten state-of-the-art baselines regarding the metrics of ACC and AUC scores. There-

into, six baselines detect visual artifacts in a single modality fashion, namely, Xception [41], F<sup>3</sup>-Net [40], Capsule [32], Meso-4 and MesoInception-4 [1], and CViT [48]. Emotional Forensics [30], and {2+1}-streams [52] are proposed to identify fake videos with multi-modal information. And the remaining two baselines, i.e., Face X-ray [25] and LipForensics [14], are models for cross-dataset detection.

### 4.4. Performance Comparison

We utilized two settings, namely within- and cross-dataset, to evaluate the proposed VFD on deepfake detection. In the former, we reported the performance of within-dataset methods, i.e., the six single and two multi-modality ones, which are trained and tested on the same dataset. As for the latter, we reproduced three within-dataset methods in a cross-dataset fashion: training on FF++ and testing on DFDC and FakeAVCeleb. Moreover, we also reported the performance of the remaining two cross-dataset approaches, i.e., Face X-ray and LipForensics. Note that we did not fine-tune our VFD over downstream deepfake datasets, i.e., VFD is agnostic to data statistics. Therefore, the VFD performance is the same for both within- and cross-dataset evaluations.

#### 4.4.1 Within-dataset Evaluation

The results of baselines and our methods under within-dataset setting are demonstrated in Table 1. It can be observed that VFD achieves a new state-of-the-art on both datasets, expressing the superiority of our method as well as the validity of tackling deepfake detection using the voice-face matching view. In addition, most single-modality models perform unfavorably, with F<sup>3</sup>-Net's accuracy less than 80% and Meso-4's around 50%. One possible reason for this is that the single-modality approaches rely heavily on the artifacts extraction capability of the backbones. Hence some strong models are prone to fail on latest data with more realistic visual artifacts, while models like CViT perform well since they employ elaborated feature extraction networks. By contrast, the multi-modal methods, namely Emotional Forensics and {2+1}-streams, can outperform the single-modality ones. We attributed this phenomenon to the fact that multiple modalities are complementary to each other, whereby the detection capability can be further enhanced.

#### 4.4.2 Cross-dataset Evaluation

We further tested the results of VFD and baselines under the cross-dataset setting. Specifically, we reproduced three traditional within-dataset approaches, i.e., Xception, F<sup>3</sup>-Net, and CViT, training them on FF++ dataset and testing on DFDC and FakeAVCeleb. As for the cross-dataset approaches, we reproduced three settings of Face X-ray and

Model	Modality		DFDC		FakeAVCeleb	
	Visual	Audio	ACC	AUC	ACC	AUC
Xception <sup>‡</sup>	✓	×	81.34	82.37	85.67	88.19
F <sup>3</sup> -Net <sup>‡</sup>	✓	×	74.36	75.70	81.08	84.54
Capsule <sup>‡</sup>	✓	×	57.65	61.20	73.27	76.19
Meso-4 <sup>‡</sup>	✓	×	49.23	52.92	43.65	49.17
MesoInception-4 <sup>‡</sup>	✓	×	56.37	60.56	72.22	75.82
CViT <sup>‡</sup>	✓	×	91.51	94.70	89.75	91.42
Emotional Forensics	✓	✓	-	84.40	-	-
{2+1}-streams	✓	✓	91.01	96.29	-	-
{2+1}-streams+att	✓	✓	90.84	95.98	-	-
{2+1}-streams+Fix-indp-audio	✓	✓	90.33	96.32	-	-
{2+1}-streams+att+ Fix-indp-audio	✓	✓	90.40	96.29	-	-
VFD	✓	✓	<b>96.19</b>	<b>98.45</b>	<b>95.07</b>	<b>96.72</b>

Table 1. Performance (%) of VFD and baselines on DFDC and FakeAVCeleb under the within-dataset setting. <sup>‡</sup>: the model is reproduced by ourselves; -: the authors did not report this metric on this dataset.

utilized the reported performance of LipForensics in the original paper. Table 2 lists the results of this experiment.

From this table, we can see that the performance of within-dataset approaches degrades significantly. F<sup>3</sup>-Net’s AUC decreases 30% on FakeAVCeleb, while Xception and CViT degrade more than 35% and 25% on DFDC, respectively, indicating the inferiority of these methods to handle unknown data. Besides, the cross-dataset methods demonstrate more advantages. For example, Face X-ray models surpass Xception on FakeAVCeleb under two settings, and LipForensics outperforms other baselines on DFDC. Moreover, VFD performs the best over all the baselines with a large margin, e.g., 25% improvement over LipForensics. It is worth noting that VFD does not apply any additional auxiliary data, which makes it different from other baselines and serves as an extra merit.

#### 4.5. Qualitative Results

To qualitatively compare our method with baselines, we demonstrated some generated heatmaps from DFDC and FakeAVCeleb in Figure 6. One can observe in Figure 6a that compared with Xception, VFD focuses on the whole face of targets, indicating that VFD recognizes fake videos based on global identity information rather than specific region artifacts. Moreover, Figure 6b illustrates more VFD heatmaps in FakeAVCeleb. It can be seen that VFD yields stable attention regions on different datasets, which further proves that VFD has a strong generalization capability and will not fail due to the migration of datasets or the update of deepfake algorithms.

Furthermore, we computed the voice-face distances from VFD via Equation (7) and showed the results in Figure 7. It demonstrates that the real and fake videos are evidently split. In addition, The split line of real and fake videos is around 300 for both datasets, implying that VFD does not

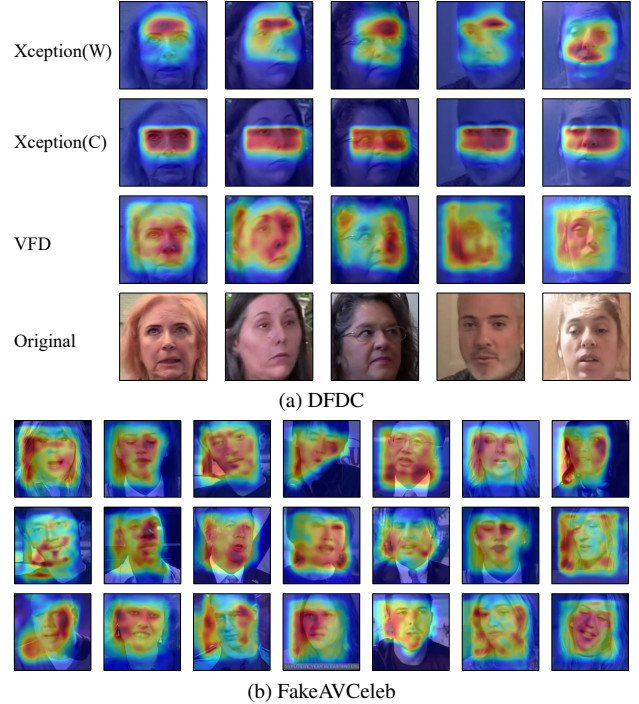


Figure 6. Heatmaps produced by baselines and our method. (a) The top two rows are from Xception trained under the within- and cross-dataset settings, followed by the third row of heatmaps yielded by our VFD and the original face images. (b) Non-cherry-picked heatmaps of VFD on the FakeAVCeleb dataset.

calculate the distance via specific features of the dataset but from the general matching view. Otherwise, different cut-off values will be learned by our method.

#### 4.6. Ablation Study

To study the effectiveness of different modules in VFD, we explored the performance of the following variants: 1)

Model	Cross-dataset	DFDC		FakeAVCeleb	
		ACC	AUC	ACC	AUC
Xception <sup>‡</sup>	×	45.95	60.51	65.03	77.20
F <sup>3</sup> -Net <sup>‡</sup>	×	57.84	60.29	35.73	53.49
CViT <sup>‡</sup>	×	61.79	68.26	70.87	73.64
Face X-ray (HRNet-18-BI100K) <sup>‡</sup>	✓	43.42	59.36	73.52	72.88
Face X-ray (HRNet-18-BI500K) <sup>‡</sup>	✓	44.80	58.98	75.65	77.94
Face X-ray (HRNet-32-BI100K) <sup>‡</sup>	✓	46.49	61.57	76.75	79.72
LipForensics	✓	-	73.50	-	-
VFD	✓	<b>96.19</b>	<b>98.45</b>	<b>95.07</b>	<b>96.72</b>

Table 2. Performance (%) of baselines and our method over the cross-dataset setting.

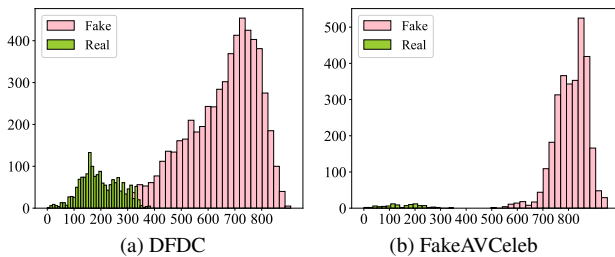


Figure 7. The distance between voices and faces. The x-axis represents the distances, and the y-axis is the number of videos.

w/o PL removes the topic pattern and latent representation matrices in Equation (2); 2) w/o MMR discards the multi-modal representation module; 3) w/o Trans. replaces the transformer-based IFL module with a standard CNN-based one; 4) w/o IFL deletes the identity feature learning module.

As can be seen from Table 3, all these four variants will jeopardize the performance to some extent. Among them, the pattern and latent matrices show the marginal influence on the final result since the remaining convolutional block can learn some contextual information. When the MMR module is eliminated, the performance will drop significantly. Furthermore, one can see that IFL module contributes most to the final performance improvement, wherein the self-attention transformer block is the crucial constitutes. We attributed this result to that transformer blocks extract the identity features from a non-local angle with more robustness, whereby the homogeneity of voices and faces can be better modeled. In a nutshell, when combining all the devised modules, our method can achieve the best result.

## 5. Conclusion and Discussion

Detecting forgery videos in deepfake is challenging due to the continuous progress from deepfake techniques. In this work, we have empirically recognized the severe mis-

Model	ACC	AUC
VFD	<b>96.19</b>	<b>98.45</b>
w/o PL	94.17	96.36
w/o MMR	88.08	91.19
w/o Trans.	88.41	92.06
w/o IFL	87.05	89.67

Table 3. Performance of VFD under different ablation settings on DFDC.

match of the voices and faces in deepfake videos, based on which we proposed to tackle this task from an unexplored homogeneity modeling perspective. In particular, our proposed method follow a Siamese-like pipeline, wherein the voices and faces from a single identity are learned to closely match. It is trained on a generic audio-visual dataset and transferred to deepfake data without any fine-tuning. When comparing with the existing elaborately designed competitors, our method achieves a significant performance improvement, thereby obtains a new state-of-the-art over two widely explored benchmarks.

Despite its effectiveness on existing deepfake datasets, VFD shows a certain limitation in the unusual case where both voices and faces are maliciously edited. Given the fact that our method addresses deepfake detection from either face swapping or voice editing, simultaneously performing these two may lead to the matching collapse. However, to the best of our knowledge, no such high-quality datasets, as well as associated approaches, have been studied in literature so far. Yet, this challenging setting is still promising and demands extensive exploration in the future.

**Acknowledgments** This work is supported by the National Natural Science Foundation of China, No.:U1936203.

## References

- [1] Darius Afchar, Vincent Nozick, Junichi Yamagishi, and Isao Echizen. Mesonet: a compact facial video forgery detection network. In *International Workshop on Information Forensics and Security*, pages 1–7. IEEE, 2018. 6
- [2] Dmitri Bitouk, Neeraj Kumar, Samreen Dhillon, Peter N. Belhumeur, and Shree K. Nayar. Face swapping: automatically replacing faces in photographs. *ACM Transactions on Graphics*, 27(3):1–8, 2008. 2
- [3] Volker Blanz, Kristina Scherbaum, Thomas Vetter, and Hans-Peter Seidel. Exchanging faces in images. *Computer Graphics Forum*, 23(3):669–676, 2004. 2
- [4] Ken Chatfield, Karen Simonyan, Andrea Vedaldi, and Andrew Zisserman. Return of the devil in the details: Delving deep into convolutional nets. In *British Machine Vision Conference*, pages 1–12. BMVA Press, 2014. 3
- [5] Harry Cheng, Yangyang Guo, Jianhua Yin, Haonan Chen, Jiafang Wang, and Liqiang Nie. Audio-driven talking video frame restoration. *IEEE Transactions on Multimedia*, pages 1–1, 2021. 3
- [6] Kai Cheng, Xin Liu, Yiu-ming Cheung, Rui Wang, Xing Xu, and Bineng Zhong. Hearing like seeing: Improving voice-face interactions and associations via adversarial deep semantic matching network. In *ACM International Conference on Multimedia*, pages 448–455. ACM, 2020. 3
- [7] Joon Son Chung, Arsha Nagrani, and Andrew Zisserman. Voxceleb2: Deep speaker recognition. In *Conference of the International Speech Communication Association*, pages 1086–1090. ISCA, 2018. 2, 4, 5
- [8] Brian Dolhansky, Joanna Bitton, Ben Pflaum, Jikuo Lu, Russ Howes, Menglin Wang, and Cristian Canton-Ferrer. The deepfake detection challenge dataset. *CoRR*, pages 1–13, 2020. 1, 4
- [9] Alexey Dosovitskiy, Lucas Beyer, Alexander Kolesnikov, Dirk Weissenborn, Xiaohua Zhai, Thomas Unterthiner, Mostafa Dehghani, Matthias Minderer, Georg Heigold, Sylvain Gelly, Jakob Uszkoreit, and Neil Houlsby. An image is worth 16x16 words: Transformers for image recognition at scale. In *International Conference on Learning Representations*, pages 1–12. OpenReview.net, 2021. 5
- [10] Jianzhu Guo, Xiangyu Zhu, Chenxu Zhao, Dong Cao, Zhen Lei, and Stan Z. Li. Learning meta face recognition in unseen domains. In *Conference on Computer Vision and Pattern Recognition*, pages 6162–6171. IEEE, 2020. 4
- [11] Yangyang Guo, Liqiang Nie, Zhiyong Cheng, Feng Ji, Ji Zhang, and Alberto Del Bimbo. Advqa: Overcoming language priors with adapted margin cosine loss. In *International Joint Conference on Artificial Intelligence*, pages 708–714. ijcai.org, 2021. 3
- [12] Yangyang Guo, Liqiang Nie, Zhiyong Cheng, Qi Tian, and Min Zhang. Loss re-scaling VQA: revisiting the language prior problem from a class-imbalance view. *IEEE Transactions on Image Processing*, 31:227–238, 2022. 3
- [13] Raia Hadsell, Sumit Chopra, and Yann LeCun. Dimensionality reduction by learning an invariant mapping. In *Conference on Computer Vision and Pattern Recognition*, pages 1735–1742. IEEE, 2006. 4
- [14] Alexandros Haliassos, Konstantinos Vougioukas, Stavros Petridis, and Maja Pantic. Lips don’t lie: A generalisable and robust approach to face forgery detection. In *Conference on Computer Vision and Pattern Recognition*, pages 5039–5049. IEEE, 2021. 2, 3, 5, 6
- [15] Elad Hoffer and Nir Ailon. Deep metric learning using triplet network. In *Similarity-Based Pattern Recognition*, pages 84–92. Springer, 2015. 2, 4, 5
- [16] Shota Horiguchi, Naoyuki Kanda, and Kenji Nagamatsu. Face-voice matching using cross-modal embeddings. In *ACM International Conference on Multimedia*, pages 1011–1019. ACM, 2018. 3
- [17] Miyuki Kamachi, Harold Hill, Karen Lander, and Eric Vatikiotis-Bateson. ‘putting the face to the voice’: Matching identity across modality. *Current Biology*, 13(19):1709–1714, 2003. 3
- [18] Ira Kemelmacher-Shlizerman. Transfiguring portraits. *ACM Transactions on Graphics*, 35(4):94:1–94:8, 2016. 1
- [19] Hasam Khalid, Shahroz Tariq, and Simon S. Woo. Fakeavceleb: A novel audio-video multimodal deepfake dataset. *CoRR*, pages 1–14, 2021. 2, 4
- [20] Hyeonwoo Kim, Pablo Garrido, Ayush Tewari, Weipeng Xu, Justus Thies, Matthias Nießner, Patrick Pérez, Christian Richardt, Michael Zollhöfer, and Christian Theobalt. Deep video portraits. *ACM Transactions on Graphics*, 37(4):163:1–163:14, 2018. 2
- [21] Diederik P. Kingma and Jimmy Ba. Adam: A method for stochastic optimization. In *International Conference on Learning Representations*, pages 1–15. OpenReview.net, 2015. 6
- [22] Pavel Korshunov and Sébastien Marcel. Speaker inconsistency detection in tampered video. In *European Signal Processing Conference*, pages 2375–2379. IEEE, 2018. 3
- [23] Mohammad Rami Koujan, Michail Christos Doukas, Anastasios Roussos, and Stefanos Zafeiriou. Head2head: Video-based neural head synthesis. In *International Conference on Automatic Face and Gesture Recognition*, pages 16–23. IEEE, 2020. 1
- [24] Lingzhi Li, Jianmin Bao, Hao Yang, Dong Chen, and Fang Wen. Advancing high fidelity identity swapping for forgery detection. In *Conference on Computer Vision and Pattern Recognition*, pages 5073–5082. IEEE, 2020. 2
- [25] Lingzhi Li, Jianmin Bao, Ting Zhang, Hao Yang, Dong Chen, Fang Wen, and Baining Guo. Face x-ray for more general face forgery detection. In *Conference on Computer Vision and Pattern Recognition*, pages 5000–5009. IEEE, 2020. 2, 3, 6
- [26] Yuezun Li, Xin Yang, Pu Sun, Honggang Qi, and Siwei Lyu. Celeb-df: A large-scale challenging dataset for deepfake forensics. In *Conference on Computer Vision and Pattern Recognition*, pages 3204–3213. IEEE, 2020. 1
- [27] Honggu Liu, Xiaodan Li, Wenbo Zhou, Yuefeng Chen, Yuan He, Hui Xue, Weiming Zhang, and Nenghai Yu. Spatial-phase shallow learning: Rethinking face forgery detection in frequency domain. In *Conference on Computer Vision and Pattern Recognition*, pages 772–781. IEEE, 2021. 1, 2

- [28] Iacopo Masi, Aditya Killekar, Royston Marian Mascarenhas, Shenoy Pratik Gurudatt, and Wael AbdAlmageed. Two-branch recurrent network for isolating deepfakes in videos. In *European Conference on Computer Vision*, pages 667–684. Springer, 2020. 1, 2
- [29] Qiang Meng, Shichao Zhao, Zhida Huang, and Feng Zhou. Magface: A universal representation for face recognition and quality assessment. In *Conference on Computer Vision and Pattern Recognition*, pages 14225–14234. IEEE, 2021. 4
- [30] Trisha Mittal, Uttaran Bhattacharya, Rohan Chandra, Aniket Bera, and Dinesh Manocha. Emotions don’t lie: An audio-visual deepfake detection method using affective cues. In *ACM International Conference on Multimedia*, pages 2823–2832. ACM, 2020. 1, 3, 6
- [31] Arsha Nagrani, Samuel Albanie, and Andrew Zisserman. Seeing voices and hearing faces: Cross-modal biometric matching. In *Conference on Computer Vision and Pattern Recognition*, pages 8427–8436. IEEE, 2018. 2, 3, 5
- [32] Huy H. Nguyen, Junichi Yamagishi, and Isao Echizen. Capsule-forensics: Using capsule networks to detect forged images and videos. In *International Conference on Acoustics, Speech and Signal Processing*, pages 2307–2311. IEEE, 2019. 6
- [33] Liqiang Nie, Mengzhao Jia, Xuemeng Song, Ganglu Wu, Harry Cheng, and Jian Gu. Multimodal activation: Awakening dialog robots without wake words. In *International ACM SIGIR Conference on Research and Development in Information Retrieval*, pages 491–500. ACM, 2021. 5
- [34] Yuval Nirkin, Yosi Keller, and Tal Hassner. FSGAN: subject agnostic face swapping and reenactment. In *International Conference on Computer Vision*, pages 7183–7192. IEEE, 2019. 1
- [35] Tae-Hyun Oh, Tali Dekel, Changil Kim, Inbar Mosseri, William T. Freeman, Michael Rubinstein, and Wojciech Matusik. Speech2face: Learning the face behind a voice. In *Conference on Computer Vision and Pattern Recognition*, pages 7539–7548. IEEE, 2019. 2, 3
- [36] Olga Papadopoulou, Markos Zampoglou, Symeon Papadopoulos, and Yiannis Kompatsiaris. Web video verification using contextual cues. In *International Workshop on Multimedia Forensics and Security*, page 6–10. ACM, 2017. 3
- [37] Omkar M. Parkhi, Andrea Vedaldi, and Andrew Zisserman. Deep face recognition. In *British Machine Vision Conference*, pages 41.1–41.12. BMVA Press, 2015. 4
- [38] K. R. Prajwal, Rudrabha Mukhopadhyay, Vinay P. Namboodiri, and C. V. Jawahar. A lip sync expert is all you need for speech to lip generation in the wild. In *ACM International Conference on Multimedia*, pages 484–492. ACM, 2020. 1, 2
- [39] Albert Pumarola, Antonio Agudo, Aleix M. Martínez, Alberto Sanfeliu, and Francesc Moreno-Noguer. Ganimation: One-shot anatomically consistent facial animation. *International Journal of Computer Vision*, 128(3):698–713, 2020. 1
- [40] Yuyang Qian, Guojun Yin, Lu Sheng, Zixuan Chen, and Jing Shao. Thinking in frequency: Face forgery detection by mining frequency-aware clues. In *European Conference on Computer Vision*, pages 86–103. Springer, 2020. 1, 2, 6
- [41] Andreas Rössler, Davide Cozzolino, Luisa Verdoliva, Christian Riess, Justus Thies, and Matthias Nießner. Faceforensics++: Learning to detect manipulated facial images. In *International Conference on Computer Vision*, pages 1–11. IEEE, 2019. 1, 2, 6
- [42] Yaniv Taigman, Ming Yang, Marc’Aurelio Ranzato, and Lior Wolf. Deepface: Closing the gap to human-level performance in face verification. In *Conference on Computer Vision and Pattern Recognition*, pages 1701–1708. IEEE, 2014. 4
- [43] Laurens van der Maaten and Geoffrey Hinton. Visualizing data using t-sne. *Journal of Machine Learning Research*, 9(86):2579–2605, 2008. 4
- [44] Ashish Vaswani, Noam Shazeer, Niki Parmar, Jakob Uszkoreit, Llion Jones, Aidan N. Gomez, Lukasz Kaiser, and Illia Polosukhin. Attention is all you need. In *Conference on Neural Information Processing Systems*, pages 5998–6008. Curran Associates, 2017. 5
- [45] Yuhang Wang, Xu Chen, Junwei Zhu, Wenqing Chu, Ying Tai, Chengjie Wang, Jilin Li, Yongjian Wu, Feiyue Huang, and Rongrong Ji. Hiface: 3d shape and semantic prior guided high fidelity face swapping. In *International Joint Conference on Artificial Intelligence*, pages 1136–1142. ijcai.org, 2021. 2
- [46] Yinwei Wei, Xiang Wang, Weili Guan, Liqiang Nie, Zhouchen Lin, and Baoquan Chen. Neural multimodal cooperative learning toward micro-video understanding. *IEEE Transactions on Image Processing*, 29:1–14, 2019. 3
- [47] Peisong Wen, Qianqian Xu, Yangbangyan Jiang, Zhiyong Yang, Yuan He, and Qingming Huang. Seeking the shape of sound: An adaptive framework for learning voice-face association. In *Conference on Computer Vision and Pattern Recognition*, pages 16347–16356. IEEE, 2021. 3
- [48] Deressa Wodajo and Solomon Atnafu. Deepfake video detection using convolutional vision transformer. *CoRR*, pages 1–9, 2021. 6
- [49] Xi Wu, Zhen Xie, YuTao Gao, and Yu Xiao. Sstnet: Detecting manipulated faces through spatial, steganalysis and temporal features. In *International Conference on Acoustics, Speech and Signal Processing*, pages 2952–2956. IEEE, 2020. 1, 2
- [50] Xin Yang, Yuezun Li, and Siwei Lyu. Exposing deep fakes using inconsistent head poses. In *International Conference on Acoustics, Speech and Signal Processing*, pages 8261–8265. IEEE, 2019. 3
- [51] Hanqing Zhao, Wenbo Zhou, Dongdong Chen, Tianyi Wei, Weiming Zhang, and Nenghai Yu. Multi-attentional deepfake detection. In *Conference on Computer Vision and Pattern Recognition*, pages 2185–2194. IEEE, 2021. 1, 3
- [52] Yipin Zhou and Ser-Nam Lim. Joint audio-visual deepfake detection. In *International Conference on Computer Vision*, pages 14800–14809. IEEE, 2021. 3, 6
- [53] Jun-Yan Zhu, Taesung Park, Phillip Isola, and Alexei A. Efros. Unpaired image-to-image translation using cycle-consistent adversarial networks. In *International Conference on Computer Vision*, pages 2242–2251. IEEE, 2017. 6